Techniques to Measure Magnetic Domain Structures

R. J. Celotta, J. Unguris, M. H. Kelley, and D. T. Pierce

National Institute of Standards and Technology, Gaithersburg, Maryland 20899

Tel: 301-975-3710
Fax: 301-926-2746

robert.celotta@nist.gov

June 16, 1999

[computer file is Word97 written in IBM DOS Format, 1.44 MB Disk]

Unit Introduction

Critical to understanding the magnetic properties and the technological application of magnetic materials is the ability to observe and measure magnetic domain structure. The measurement challenge is quite varied. Magnetic fluids can be used to decorate and make simple domain structures visible while highly sophisticated electron microscopy based methods may be needed to explore and image nanometer scale magnetic phenomena. No one method will solve all of the important domain imaging problems. For that reason, we will discuss the bases of all the important methods and the practical implications of each.

For purposes of comparison, several important characteristics of each domain imaging technique we discuss are briefly summarized in Table 1. However, the table should only be used as a broad outline of the different methods and any choice of method should include the relevant sections below and the references therein.

There are several general comments that apply to every domain imaging method we discuss. First, each method is related either to a sample's magnetization or to the magnetic field generated by that magnetization. The former is of great usefulness in understanding or developing new materials and the latter is of practical importance in devices. Second, all of the methods are limited to the topmost few micrometers and are therefore dominated by magnetic structure related to the surface. None provide the domain structure of the interior of a thick sample where bulk magnetic microstructure is fully developed. Third, all of the methods require smooth, clean, damage-free surfaces. In general, the surfaces need to have at least the equivalent of a mirror polish. Otherwise, topography and surface stress will affect the measurement to varying degrees.

Fourth, correlations exist between several of the parameters in each technique we describe. For example, it may not be possible to achieve the ultimate sensitivity specified at the highest resolution possible. Finally, almost all of the techniques use digital signal acquisition and can benefit from the use of modern image processing tools.

What follows are expanded discussions of the basis of each technique, its practical aspects, sample preparation required, sample modifications that are possible, and problems that are specific to the technique described. Each section contains references to more complete treatments of the technique and recent examples of its use.

Bitter Pattern Imaging

Principles of the Method

Bitter or powder pattern imaging of domain structures is arguably the oldest domain imaging technique, and still probably the simplest method to apply. In Bitter pattern imaging a thin colloidal suspension of magnetic particles is painted on a magnetic surface. The particles collect and agglomerate in regions where large stray fields from the sample are present, typically over domain walls. The decorated domain walls can then be imaged using an optical microscope, or, if higher resolution is required, an electron microscope. Figure 1 shows an example of a Bitter pattern image of bits written on a magnetic hard disc.

The Bitter technique is strictly a stray field decoration technique. The patterns provide no information about the magnitude or direction of the magnetization, but in materials with

sufficiently large external fields, Bitter patterns can quickly provide information about the size

and shape of any domains that may be present. Bitter pattern imaging has been reviewed by

Kittel and Galt (1956) and Craik (1974).

Practical Aspects of the Method

The resolution of the Bitter method primarily depends both on the size of the individual or

agglomerated particles in the colloid, and the resolution of the microscope used to image the

patterns. Historically a researcher had to be skilled in the preparation of Bitter solutions, but

today there are several commercial suppliers of Bitter solution colloids, sometimes referred to as

ferrofluids (Ferrofluids from Ferrofluidics Corp., Nashua, New Hampshire and Lignosite FML

from Georgia Pacific Corp., Tacoma, Washington). By selecting the appropriate Bitter solution,

these commercial ferrofluids can reveal magnetic structures down to the resolution limit of the

optical microscope. Higher resolutions can be attained by imaging the decorated sample with a

scanning electron microscope (Goto and Sakurai, 1977), or by using fine grained sputter

deposited films for decoration (Kitakami, et al., 1996).

Contrast in the Bitter method depends on sufficiently large stray magnetic field gradients to

collect the magnetic particles. Although certain ferrofluids can be sensitive to stray fields as

small as a few hundred A/m, the stray fields outside of some high permeability or low anisotropy

materials may still be too small to image. For this reason, the technique generally works better

with higher coercivity magnets or perpendicularly magnetized samples. In fact, a small

perpendicular applied magnetic field is frequently used to improve the contrast. As with any

magnetic field sensitive domain imaging technique, deriving the magnetic structure from the

observed Bitter pattern image can be difficult, since the external magnetic fields may be the result of non-local variations in the sample's magnetization.

Sample Preparation

The Bitter method requires some sample preparation, because the technique does not separate the magnetic from the topographic contrast. Bulk samples are usually prepared by mechanically polishing the surface, followed by chemical or electropolishing to remove residual surface strains. Thin films deposited on polished substrates can also be used. Aside from the smoothness, there are few constraints on the types of magnets that can be studied. The samples can be conductors or insulators, and thin non-magnetic coatings are allowed. On the downside, the ferrofluid can contaminate the surface, leaving behind residues which may not be easily removed.

Specimen Modification

As long as the magnetic particles remain in solution, the Bitter pattern can be used to examine the motion of domains and domain walls while applying a magnetic field. The response time of the ferrofluid may be rather slow, however, due to the viscosity of the colloid. In some cases it may take several minutes for the Bitter pattern to come to complete equilibrium. The ability to observe domain wall motion while applying a magnetic field is essential when trying to separate magnetic structure from sample topography.

Magneto-optic Imaging

Principles of the Method

The weak interaction between polarized light and a material's magnetization leads to several

useful optical domain imaging methods (Craik, 1974) Although the physics of the magneto-optic interactions can be rather complicated (Hubert and Schäfer, 1998), at the most basic level magneto-optic imaging is simply based on the rotation of the plane of polarization of linearly polarized light upon reflection from, or transmission through a magnetic material. In transmission, the magneto-optic effect is usually referred to as the Faraday effect, and in reflection as the Kerr effect. In both cases the domain contrast in the image is directly related to the magnitude and direction of the magnetization in the sample.

Practical Aspects of the Method

The relative geometry between the magnetization direction and the direction of the transmitted or reflected light determines which component of the magnetization vector will be visible in a particular magneto-optic image. When light is incident normal to the sample surface in either the "polar" Faraday or Kerr mode, domains that are magnetized perpendicular to the surface are imaged. In-plane magnetization can be detected in the Faraday or Kerr modes using oblique illumination. In the longitudinal Kerr effect the in-plane magnetization component lies in the scattering plane of the light, while in the transverse Kerr effect the magnetization is perpendicular to the scattering plane. Contrast in the polar mode is greatest at an angle of incidence of 0° while the longitudinal and transverse Kerr effects are greatest at about 60° angle of incidence.

Typically magneto-optic images can be generated either by using conventional imaging optics or by rastering a finely focused laser spot across the sample surface. In either case high quality strain-free optics and polarizers with high extinction ratios are preferred, because the magneto-

optic effects are quite small. The Faraday and polar Kerr modes provide the most contrast, while

the contrast in the longitudinal Kerr mode is so small that additional electronic signal processing

is usually required to separate the magnetic contrast from the non-magnetic background

(Schmidt, et al., 1985; Argyle, 1990; Trouilloud, et al., 1994).

The resolution of the magneto-optic image is determined by the resolution of the optical imaging

system or, in the case of rastered laser imaging, by the size of the focused laser spot. Typical

resolution is therefore about 1 μm, but can be improved to 0.3 μm in a high quality optical

microscope using an oil immersion objective and blue light illumination. Further improvements

in resolution can be achieved by using various forms of scanned near-field optical imaging, but

the contrast mechanisms in these methods are not yet well understood (Betzig, et al., 1992; Silva

and Schultz, 1996). The sampling depth in the Kerr imaging mode is determined by the

penetration depth of the light and is about 20 nm in a metal. Therefore, the technique is

moderately surface sensitive and can be used to image magnetic domains in thin films that are

only a few monolayers thick, as well as to image domains that are covered by sufficiently thin

films of materials that are normally opaque.

Sample Preparation

The small sampling depth and topographic sensitivity of the Kerr imaging mode requires

preparing samples that have optically flat, damage free surfaces. Bulk samples can be prepared

by mechanical polishing, followed by chemical polishing or annealing to remove the remaining

damage. High quality surfaces for imaging can also be generated by evaporation or

electrodeposition of thin films on flat, polished substrates. Samples may be coated by thin,

nonmagnetic films, without significantly affecting the magneto-optic images. In fact, appropriate antireflective coatings can be applied to samples in order to increase the magneto-optical contrast.

Specimen Modification

Perhaps the greatest advantage of magneto-optic imaging is the speed with which magnetic images can be acquired. Video rate imaging of domain dynamics is routinely achieved using standard arc lamp illumination. Stroboscopic imaging using pulsed laser illumination can reveal domain wall motion that occurs over time scales as short as a few nanoseconds (Petek, et al., 1990; Du, et al., 1997). In fact magneto-optic imaging can yield a great deal of information about magnetization dynamics in a magnetic material or device, since arbitrarily large magnetic fields may be applied to the sample while imaging. Figure 2 shows a magneto-optic image of a thin film recording head. This image highlights the domain wall motion within the head by taking the difference between images with the current in the head coils reversed.

Problems

The major difficulty with the Kerr imaging mode is having to separate the magnetic image from a potentially larger non-magnetic background and from the intensity variations due to the sample's topography. Various approaches have been used to improve the contrast and eliminate topographic feed-through. Antireflective coatings may be applied to the sample (Hubert and Schäfer, 1998). The fact that the sense of the Kerr rotation is independent of the direction of incidence may also be exploited by using wide angle illumination and a segmented optical detector (Silva and Kos, 1997). The most common method is to measure, using sufficiently

precise instrumentation, the difference between the images taken before and after a magnetic field is applied to reverse the magnetization. In practical terms this means that magneto-optic imaging is best applied to samples where the magnetization may be changed by applying a field, such as in the thin film magnetic recording head shown in Fig. 2. On the other hand, high quality images of static magnetic domain patterns which one cannot or does not want to alter, such as written bits in recording media, are difficult to acquire.

Finally, there are several new developments in magneto-optical imaging that are worth noting because of their potential future impact. First of all, nearfield optical techniques are being used to overcome the resolution limits of conventional diffraction limited optics. By using scanned apertures or tips in close proximity to a surface, resolutions on the order of $\lambda/10$ have been achieved (Betzig, et al., 1992; Silva and Schultz, 1996). Second, magneto-optic indicator films have been developed as an alternative to Bitter pattern imaging (Nikitenko, et al., 1996). In this method a thin, free-standing garnet film is placed against a magnetic sample and the resulting domain pattern, induced by the sample's stray field, is imaged using a conventional polarized light microscope. Compared with Bitter imaging, this relatively simple and inexpensive technique has the advantage of faster response to applied magnetic fields and no sample contamination. Finally, intense laser illumination has made imaging using second harmonic Kerr effects possible (Kirilyuk, et al., 1997). The second harmonic effects result from the nonlinear optical response of certain materials, enabling this mode to image structures, such as domains in antiferromagnets, that are not visible with conventional Kerr imaging.

Magnetic Force Microscopy (MFM)

Principles of the Method

Magnetic Force Microscopy (MFM) has become one of the most widespread tools for studying the magnetic structure of ferromagnetic samples and superconductors (Rugar and Hansma, 1990; Sarid, 1991). The technique is based on the forces between a very small ferromagnetic tip attached to a flexible cantilever and the inhomogeneous stray magnetic field immediately outside a sample of interest. As the magnetic tip is scanned over a magnetic sample, these minute forces are sensed in any of a variety of ways to provide maps related to the magnetic field above the sample.

In the implementation of an MFM, there are a very large number of choices to be made which influence, in a fundamental way, how the observed image should be related to the magnetic field. For example, an MFM in which the tip is magnetically relatively soft (i.e., the tip magnetization is modified by its interaction with the sample) provides a very different image of the magnetic field than one which utilizes a tip which is magnetically relatively hard (i.e., the tip magnetization does not change in response to the magnetic field of the sample). Similarly, the distribution of magnetic moments in the tip can have a pronounced qualitative effect on the imaging. Whereas a point-like magnetic particle on the tip may be best modeled as a simple magnetic dipole, a tip which is longer or more like a needle may be best modeled as a magnetic monopole. Further, the MFM may sense either the net deflection of the tip in the field of the sample or may sense changes in either the amplitude, frequency, or phase of the vibrational motion of a tip oscillating resonantly in the field above the sample. One direct result of the complex and multi-faceted interaction between the tip and sample is that it is very difficult to determine the field distribution from an MFM image.

Because of the huge number of possible implementations implied by these (and many other) available choices, and further because the state-of-the-art for magnetic force microscopy is currently being developed very rapidly in numerous laboratories, it is not possible in the current context to provide a thorough or complete report on the status of magnetic force microscopy. Instead, we will present a general description of an MFM in one form readily available commercially.

Rather than directly sensing the deflection of the flexible cantilever due to magnetic forces acting on the magnetic cantilever tip, MFMs typically detect changes in the resonant vibrational frequency of the cantilever. In this mode of operation, the cantilever is electrically driven to oscillate, with the driving frequency controlled to track very precisely the resonant vibrational frequency of the cantilever. When they are in close proximity, the scanning tip and sample surface generally experience an attractive net force (e.g., from Van der Waals interactions). In addition to this attractive force will be a force of magnetic origin which will be either attractive or repulsive depending on the relative orientation of the tip magnetization and the magnetic field gradients above the sample. Where the magnetic force is also attractive, the cantilever is deflected further towards the surface. This effectively stiffens the cantilever, raising its natural resonant frequency. If the magnetic force is repulsive, the cantilever is deflected less strongly towards the sample, effectively softening the cantilever and lowering its resonant frequency. Because the resonant frequency of the cantilever can be determined with very high precision, that frequency provides a convenient means by which to monitor local variations in the magnetic field gradients.

However, because the magnetic forces between tip and sample are very small, one general problem that all MFMs must address is the separation of image contrast arising from magnetic forces from the image contrast due to other (stronger) short-range physical forces (Schoenenberger, et al., 1990).

Figure 1 shows, as an inset, a magnified region of a test pattern written on magnetic storage media as imaged with a commercial Magnetic Force Microscope. The written bits are clearly visible and highlight the fact that the MFM is primarily sensitive to gradients in the magnetic field. Regions where the magnetization changes from left to right (or right to left) are visible as white (or dark) lines. This contrast would reverse with a magnetization reversal of the MFM tip.

Practical Aspects of the Method

There are several practical aspects to MFM imaging which should be noted. First, it is generally not known with confidence what underlying contrast mechanism gives rise to an MFM image. The signal is generally proportional to spatial derivatives of the stray field above the sample, but which spatial derivative in which direction depends on the details of the magnetic moment distribution within the tip, tip/sample interactions, operating mode of the MFM signal detection and control electronics, vibrational amplitude of the cantilever, and lift height of the MFM scan relative to the AFM topographic scan, etc. As a consequence, quantitative interpretation of MFM images is generally very difficult (Hug, et al., 1997). Even qualitative interpretation can sometimes be very uncertain. Because the MFM can often be configured to give contrast which is proportional to the magnetic field as well as to various spatial derivatives, one is often

uncertain whether observed magnetic contrast is due to a magnetic domain or to the domain wall between two domains. As with many scanned-tip microscopes, navigation on a sample can be difficult. The MFM always operates at very high magnification so that it can be difficult to find specific isolated features for study.

As mentioned above, the effects of surface topography can be pronounced on magnetic force microscopy. One common solution to this problem is to acquire the magnetic image in two steps. In the first step, the microscope is operated as a conventional Atomic Force Microscope (AFM; not discussed here) so as to determine in detail the topographic profile along one scan line. The microscope then retracts the tip and, using the previously determined line profile, rescans the same line with the magnetic tip at a small but constant height (typically 20-200 nm) above the sample. In this second scan, the longer range magnetic forces still affect the cantilevered tip, but the effect of the short range forces is minimized. This effectively provides a map only of variations in the local magnetic field, free of topographic contrast.

Even with such methods to compensate for the effects of surface topography, samples must be very smooth for these methods to be effective. Surfaces that have significant roughness or surface relief can be very difficult to image with the MFM. Sometimes the AFM prescan is not adequate because the surface relief is too great for the AFM tip positioning to be reliable. Even if the AFM topography scan is successful, other problems arise if the combination of tip vibrational amplitude and surface texturing is so large that the tip contacts the sample during the MFM scan.

One very useful feature of the MFM is that because the MFM senses the stray magnetic field rather than the sample magnetization directly, it is easy to see the magnetic structure even through relatively thick non-magnetic and even insulating overlayers.

Data Analysis and Initial Interpretation

Significant image processing is generally required to aid in the interpretation of MFM images. The relevant image processing steps are typically integrated into the commercial MFM instrument controllers. One example is the above mentioned subtraction of contrast due to surface topography. This subtraction, however, has the side-effect that domain walls which run parallel to the scan direction can be much more difficult to image than walls running at a significant angle to the scan direction.

Sample Preparation

One of the very attractive features of the MFM is that minimal surface preparation is required. Samples that are smooth and flat enough to image with an atomic force microscope can generally be studied with MFM as well.

Problems

As mentioned above, consideration must be always given to the extent to which the magnetic structure of the tip or sample is modified in response to the magnetic field of the other.

Type I and Type II Scanning Electron Microscopy

Principles of the Method

It is often possible to image the magnetic domain structure of a sample with a conventional

scanning electron microscope. Two distinct contrast mechanisms, referred to as Type I and Type

II magnetic contrast, have been described (Newbury, et al., 1986; Reimer, 1985). Both are based

on the deflection (due to the Lorentz force) of electrons moving in a magnetic field. Two

important features distinguish between Type I and Type II contrast. First, whereas Type I

contrast involves imaging low energy secondary electrons ejected from the sample, Type II

contrast arises from high energy, backscattered electrons. Second, whereas Type I contrast arises

from the deflection of the secondary electrons by stray fields outside of the sample, Type II

contrast relies on deflection of the incident and backscattered electrons by magnetic fields within

the samples.

Practical Aspects of the Method

There are relative advantages and disadvantages to both types of magnetic contrast. The primary

advantages are that no special modifications are required either for the scanning electron

microscope or the sample. Essentially any conventional scanning electron microscope can be

used for Type I contrast. The only special requirement, that may involve modification to the

secondary electron detector, is the positioning the detector to one side of the sample and

preferentially detecting secondary electrons which are ejected toward rather than away from the

detector. Some detectors have a sufficiently high bias voltage for secondary electron collection

that this differential sensitivity is inadequate to observe Type I contrast. If the microscope

includes (as is very common) a detector for backscattered electrons, then Type II contrast is also

feasible. The primary disadvantages are that spatial resolution is limited and that it is sometimes

difficult to distinguish between magnetic contrast of either type and other types of signal

contrast.

For Type I contrast to be optimized, the primary beam energy typically should be less than 10 keV in order to produce the most secondary electrons. Because contrast depends on the geometry of the microscope's electron detector relative to the sample magnetic structure, tilt and rotation control of the sample are necessary to optimize contrast. Spatial resolution is limited typically to about 1 μm due to the spatial extent of the external magnetic fields. In some circumstances, the sample tilt and rotation also allow Type I contrast to be used for quantitative imaging of the magnetic fields outside of a sample (Wells, 1983).

Type II contrast is maximized by using the highest available beam energy and by tilting the sample surface to about 50° relative to the incident beam. The contrast varies from about 0.1% at 20 keV to about 1% at 200 keV. Because the contrast is relatively low, high primary beam currents are required. The spatial resolution is then determined both by the size of the primary beam and by the escape volume of the backscattered electrons. For the direction parallel to the tilt axis, this resolution varies from about 1 μm at lower energies to about 2 μm at 200 keV. For the direction perpendicular to the tilt axis, the resolution is significantly degraded and is roughly determined by the penetration depth for the incident electron. For 200 kV electrons, that resolution is about 10 μm.

Type II magnetic contrast, of all the imaging techniques described, can have the greatest information depth. At 200 keV, the electrons penetrate about 15 μm of material, with the

maximum backscattering intensity coming from a depth of about 9 μm. Consequently, Type II is less surface sensitive than the other imaging techniques. Further, exploitation of the dependence of the penetration depth on primary beam energy provides a coarse method for magnetization depth profiling.

Data Analysis and Initial Interpretation

No significant data analysis is required, but interpretation is generally restricted to qualitative studies of domain sizes and shapes.

Sample Preparation

No special preparation required, other than polishing for the removal of topographic features which would otherwise compete with the relatively weak magnetic contrast.

Lorentz Transmission Electron Microscopy

Principles of the Method

This form of very high resolution magnetic microscopy gets its name from the Lorentz force that causes a deflection of the electron trajectory for a beam traveling perpendicular to a magnetic field. The Type I and Type II methods, described previously, also are based on the Lorentz force. However, while Type I and Type II imaging are performed on the surface of a sample in a Scanning Electron Microscope (SEM), Lorentz microscopy makes use of either a Conventional Transmission Electron Microscope (CTEM) or a Scanning Transmission Electron Microscope (STEM), and involves transmission through thinned samples. Within the general category of

Lorentz microscopy, three distinct imaging techniques (McFayden et al, 1992; Chapman, 1984) can be identified, i.e., Fresnel, Foucault, and Differential Phase Contrast (DPC) microscopy.

By using a CTEM in the Fresnel mode (Heyderman et al, 1995), narrow regions of relatively high and low intensity are formed at positions that correspond to domain walls; this results from small deflections caused by the Lorentz force acting on a defocused beam of electrons transmitted through the sample. Consider a thinned magnetic sample with a domain geometry of parallel strips with the magnetizations in each strip lying in-plane and in alternating directions parallel to the domain walls separating them. The Lorentz force will, depending on the magnetization direction of each domain, deflect the beam slightly toward one wall or the other. As a consequence, the domain will be seen to have a bright wall on one side and a dark wall on the other. Figure 3 (top) shows an example of Fresnel imaging of a metallic glass.

In the Foucault mode (Heyderman et al, 1995) using a CTEM, the image remains in focus and a diffraction pattern is formed at one of the aperture planes of the microscope. By displacing the aperture, it is possible to block electrons that have been deflected in one direction by the magnetic field. In the image subsequently formed, the brightness within each domain will depend on the direction of its magnetization. Figure 3 (bottom) shows an example of Foucault imaging.

In the DPC mode (McVitie et al, 1997), a STEM is modified by the addition of a quadrant electron detector and matching electronics. A focussed, scanning probe beam is deflected on passing through the thin sample and the extent of the Lorentz deflection is measured from the

differences and ratios of currents incident on the quadrants of the electron detector. A

quantitative measure of the magnetic field lying perpendicular to the electron's path through the

sample is possible.

Practical Aspects of the Method

These methods, particularly DPC, are capable of excellent resolution, approaching 2 nm for

magnetic structures in the best of circumstances, and 10-20 nm for more typical applications.

Physical structure can be seen with even higher resolution. Image acquisition times are typically

tens of seconds for computer controlled DPC image acquisition.

These methods are quite sensitive, being able to detect just a few layers of Fe, in cases where the

crystallographic contrast does not interfere. Since deflections are caused by the magnetic field

within the sample, the information depth is the full sample thickness with equal weighting for all

depths. Note however that magnetic fields outside the sample surface can also cause deflections

that could modify the image.

The complexity of these methods is moderately high. They all use a TEM and may involve

preparing a sample by thinning, which it should be remembered, can have an effect on the

domain structure. TEMs suitable for use in these modes are readily available commercially. The

highest resolution systems with field emission sources and a variety of attachments can cost

$1M, although the cost to add a magnetic imaging capability to an existing TEM would be much

less. In the DPC method, the electronics necessary to derive, display and store the difference

signals is not commercially available. Also, some technique must be implemented to 'descan' the

probe beam on the detector plane, i.e., remove the contribution to the differential detector signal

that comes from a scanning probe beam rather than magnetic deflection.

Method of Automation

In the DPC method, the four quadrant detectors (or eight if a scheme to separate magnetic and

non-magnetic contrast is used) are connected to preamplifiers and an amplifier/mixer to derive

multiple signals including the sum of all channels, and the sums and differences between various

quadrants. These signals are displayed in real time and filtered, digitized, and stored in a

computer for later analysis.

Data Analysis and Initial Interpretation

Images produced in the Fresnel and Foucault modes immediately display the domain walls or

domains, respectively. The dimensions of the domains can be determined quantitatively from

these images. The DPC method uses the digitized signals stored for each x, y point in the image;

the magnitude, direction, and curl of the magnetic induction can be calculated and displayed.

Additional displays including color wheel representations of direction and histograms showing

the distribution of fluctuations in direction are also readily available.

Sample Preparation

Only very thin samples can be analyzed. This method is generally applicable for samples less

than 150 nm thick. As with other electron based methods, only conductive samples can be

imaged.

Common to all the Lorentz methods described above is the requirement that the microscope does not generate sufficient magnetic field at the sample to modify the domain pattern. This problem can be addressed by either turning off the objective lens, moving the sample away from the strongest field position, or using a low field lens specifically designed for the purpose. Unfortunately, all of the solutions will degrade the spatial resolution somewhat.

Specimen Modification

Magnetic fields can be purposefully applied to the sample, so long as they do not significantly affect the operation of the microscope. In a typical case, magnetic fields can be applied to the sample if held below 500 kA/m in the direction along the microscope column and 80 kA/m perpendicular to it. Modification of the sample due to beam heating effects is usually considered negligible.

Scanning Electron Microscopy with Polarization Analysis (SEMPA)

Principles of the Method

Scanning Electron Microscopy with Polarization Analysis (SEMPA) is a magnetic imaging technique based on the measurement of the spin-polarization of secondary electrons ejected from a ferromagnetic sample by an incident beam of high-energy electrons (Scheinfein, et al., 1990). These secondary electrons have a spin polarization that is determined by their original spin polarization, i.e., the magnetization in the bulk sample. An image of the magnetic domain microstructure at the surface can thus be generated by a measurement of the secondary electron spin polarization at each point as a tightly focused electron beam is scanned in a raster fashion over a region of interest.

For a 3d transition metal such as iron, both the bulk magnetic properties and the emitted low-energy secondary electrons are dominated by the valence electrons, with remaining electrons behaving essentially like an inert core. One can, then, roughly predict the degree of secondary electron spin polarization in iron from the observed magnetic moment of atoms in the bulk (2.22 Bohr magnetons) and the number (8) of valence electrons. One expects a spin polarization of approximately $2.22/8 \approx 0.28$, in good agreement with experimental observations. Similarly, good predictions can be made for cobalt (0.19) and nickel (0.05) as well.

The polarization detectors typically used for SEMPA (Scheinfein, et al., 1990) provide simultaneous determination of the electron polarization projected onto two orthogonal axes. Frequently, those axes are parallel to the surface of the sample so that SEMPA measures the in-plane surface magnetization. SEMPA detectors can also be constructed to measure the magnetization perpendicular to the surface along with one in-plane component. However, magnetic anisotropy at the surface generally forces the magnetic moments for most samples to lie in the plane of the surface so that out-of-plane magnetization is rarely observed.

There are several general features of SEMPA that deserve particular attention in comparison with other magnetic imaging techniques. First, whereas many magnetic imaging techniques are sensitive to the magnetic fields either inside or outside of the sample, SEMPA determines the sample magnetization directly. Second, because the physical basis for magnetic contrast is well understood, the magnetic images can be quantitatively analyzed. Third, the magnetization signal

is very large. A huge number of secondary electrons are generated in a typical SEM scan and

even in a low-moment material like nickel, the magnetization signal is 5% of the total secondary

electron current. Unfortunately, as discussed below, the inherently low efficiency of spin

polarization detectors makes measurement of this large signal quite difficult. Fourth, because the

magnetic resolution is essentially given by the focused diameter of the primary electron beam,

very high spatial resolutions (~20 nm) can be achieved. Fifth, the electron polarization detector

simultaneously provides images of both the magnetization and the secondary electron intensity.

The intensity images provide information about the physical structure of the sample under study.

Hence, a comparison of the magnetic and topographic images can provide insight into the

influence of physical structure on the magnetic domain structure. Finally, because the escape

depth of low energy secondary electrons is short (few nm) SEMPA measures the magnetic

properties of the near surface region and is thus ideally suited to studies of magnetic thin films or

of magnetic properties peculiar to the surface region.

An insert in Fig. 1 shows a magnetic image of a test pattern in hard disk media as imaged by

SEMPA. The details of the magnetic structure are clearly visible, both in the recorded tracks and

in the randomly magnetized regions between the tracks.

Practical Aspects of the Method

There are several practical aspects of SEMPA which determine its applicability to specific

magnetic imaging problems. Most notably, because the attenuation length of the low-energy

secondary electrons is typically sub-nanometer, SEMPA is sensitive to only the outermost few

atomic layers. Hence, magnetic domain contrast is rapidly attenuated by nonmagnetic

overlayers. Such overlayers could be the surface lubricant of magnetic hard disk media,

protective non-magnetic capping layer of a magnetic multilayer, or merely the naturally

occurring adsorbed gases and contaminants which are always present on surfaces exposed to the

atmosphere. Prior to magnetic imaging, any nonmagnetic overlayers should be removed,

generally by ion sputtering. In order to minimize the effects of surface contamination after

cleaning, SEMPA studies must be performed under ultra-high vacuum conditions.

One very useful side effect of SEMPA's high surface sensitivity is the ability to measure the

magnetic properties of minute amounts of magnetic material. One can readily measure the

magnetic properties of iron at sub-monolayer coverages. At roughly 1 monolayer coverage, with

the primary electron beam focused into a 10 nm spot, SEMPA is measuring the magnetic

properties of only about 1000 iron atoms.

As alluded to above, one practical consideration is the inherently low efficiency of electron

polarization detectors. At present, most polarization detectors rely on differences, due to

electron spin orientation, in the cross section for scattering of the electrons under investigation

from a heavy nucleus. Both because the overall scattering probability is low and because the

difference due to electron spin is small, the overall efficiency of polarization detectors is about

10^{-4}. Consequently, data acquisition times can be quite long, depending on the intensity of the

primary electron beam and the inherent secondary electron polarization of the sample under

study.

Data Analysis and Initial Interpretation

Data analysis in SEMPA is rather straightforward. The data is collected as the magnetization

vector component along two orthogonal directions, typically in the sample plane. These

components, however, can be readily combined to generate the net magnetization

$/\mathbf{M}/= \sqrt{M_x^2 + M_y^2}$ and the magnetization direction $\left(\theta = \tan^{-1}\left(M_y / M_x\right)\right)$. While the magnetization

direction is determined uniquely, the magnitude of the magnetization is determined only to

within a constant. The absolute efficiency of most electron polarization analyzers is not known

with accuracy so that individual detectors require calibration. Further, as mentioned above, the

dependence of the secondary electron spin polarization on sample magnetization is known only

approximately. However, because both of these factors are essentially constant, it is possible to

make quantitative interpretations concerning changes in the degree of magnetization over the

sample under study.

Because the magnetization signal from electron spin polarization detectors can be very small,

instrumental artifacts can sometimes influence the magnetization images in significant ways.

However, such instrumental artifacts are generally either reduced to negligible levels or

measured and accounted for in the image analysis (Kelley, et al., 1989).

Sample Preparation

Because SEMPA measures the magnetic properties of only the outermost atomic layers, samples

should be atomically clean. The preferred method is ion sputtering. However, though the

magnetic contrast may be significantly reduced, it is sometimes possible to observe domain

structure through very thin layers. For example, one can observe domain structures essentially

unchanged through a few monolayers of gold.

The collection of low-energy secondaries and the preservation of their spin orientation severely limit the acceptable size of any magnetic fields at the sample. Typically, stray fields must be non-varying and of order or smaller than the earth's magnetic field. Apart from special sample geometries which allow nearly complete elimination of stray magnetic fields, one is essentially restricted to zero-field measurements.

Holography

Principles of the Method

Magnetic domain imaging is an important application of electron holography (Tonomura, 1994) in part because this technique makes possible both direct visualization and quantitative measurement of magnetic flux, Φ_B. In electron holography, a high energy, e.g., 200 keV, field emission, transmission electron microscope (TEM) or scanning transmission electron microscope (STEM) is used to form an interference pattern from electrons that can reach the detector via two alternative paths, one of which contains the sample specimen. The electrons can be thought of as waves emitted from a very small source with a very narrow energy distribution, i.e., the beam has high degrees of both spatial and temporal coherence. The beam is divided into two parts, using an electron biprism, with one half of the beam passing through the thin specimen to be studied while the 'reference' half of the beam continues unimpeded. When the two halves of the beam are recombined on a film detector, following electron optical magnification, an interference pattern is observed. If there were no sample, the interference pattern would consist of equally spaced parallel lines. These lines are located at positions where the length of the two

possible paths differs by an integral number of electron wavelengths. If there is a sample in one path, then the sample may introduce phase shifts in the electron wave passing through it and those phase shifts will result in a local modification of the interference pattern.

When electron holography is used for magnetic imaging (Osakabe, 1983; Tonomura, 1994; Mankos et al, 1996, 1996a), interference is observed between electron waves in the reference path and those passing through a magnetic sample. However, an additional phase shift is introduced between the two waves. This phase shift is proportional to the total magnetic flux enclosed by the two alternative electron paths. For this case, known as the absolute method, the lines in the interference pattern can be directly interpreted as flux lines. In fact, the normalization is such that a flux of 4.1 x 10^{-15} Wb, i.e., h/e, flows in the space between two adjacent contour lines. An alternative, differential mode can also be used. In this mode, both beams go through the magnetic sample with slightly different paths. The phase difference, being proportional to the flux within the path enclosed by both beams, will be constant for a uniformly magnetized material and sensitive to a region of rapid change in enclosed flux, e.g., a domain wall. Figure 4 shows the flux distribution both inside and adjacent to a strip of magnetic tape measured using the absolute method in a TEM.

Practical Aspects of the Method

Using electron holography, high spatial resolution is possible; a resolution of 10 nm has been demonstrated. Since this is a transmission method, the magnetic sample must be uniformly thinned and the information obtained will represent values averaged over a typical sample thickness of 50 nm. Samples of up to 150 nm in thickness are generally possible. One must

consider the possibility that the necessary thinning of the sample may affect the magnetization distribution in the sample being imaged. Only conductive samples can be measured. The flux enclosed in the electron path is quantitatively measured with a minimum sensitivity of about 10^{-16} Wb. The instrument used is an extension of a high quality transmission electron microscope. As such, it is a rather complex device. A commercial version designed for holography is available at a cost of about $1.3M.

Method Automation

A variety of image capture methods are available. Photographic film can be used or a CCD TV camera can provide a real time display or permit transfer of the image to video tape to record dynamic information, for example, the variation in response with a changing magnetic field.

Data Analysis and Initial Interpretation

The hologram that results from the two beam interference in a microscope equipped for electron holography is an interferogram that directly displays the changes in phase that result from the magnetic flux of the sample. A major strength of this method is that these interference fringes can be directly interpreted as representing magnetic lines of force. Occasionally, additional sensitivity is required to see small variations in the enclosed magnetic flux. In this case, the phase amplification technique (Tonomura, 1994) is used to increase, within limits set by the overall signal-to-noise ratio, the number of interference lines for a set amount of flux, i.e., to increase the sensitivity.

Sample Preparation

The sample must be uniformly thinned to <150 nm. If the absolute method is going to be used,

the sample should be prepared so that the area to be measured is either near the sample edge or a

hole in the sample through which the reference beam can pass.

Specimen Modification

It is possible to have a local magnetic field of less than 100 kA/m at the sample.

Problems

This is a complex method requiring a very significant investment in equipment, sample

preparation, and image reconstruction and analysis. It has been applied to a wide range of

problems, including small particle and multilayer magnetism, observation of domain walls and

imaging of fluxons in a superconductor.

X-Ray Magnetic Circular Dichroism (XMCD)

Principles of the Method

X-ray magnetic circular dichroism (XMCD) is a recently developed technique made possible by

the availability of intense, tunable synchrotron radiation from a new generation of storage rings.

The effect depends on the relative orientation of the x-ray photon angular momentum and the

sample magnetization. The difference in the absorption of x-rays, a phenomenon know as x-ray

dichroism, is maximum when magnetization of the material and the photon angular momentum,

or helicity, are parallel and antiparallel. The x-ray photon transfers angular momentum to the

photoelectron excited from a spin-orbit split core level. For transition metals, XMCD

measurements typically involve transitions from spin-orbit split p states (L_2 and L_3 core levels) to

valence d states which in a ferromagnet are spin polarized. The transition probability depends on

the spin orientation of the d final states and hence on the magnetization.

A key advantage of XMCD for imaging magnetic domains is the elemental specificity that

derives from the process being tied to an absorption event at a particular core level. In principle,

it is possible to correlate the magnetic measurement with other core level measurements which

give information on the local site, symmetry and chemical state. Because the spin and orbital

moments can be determined from XMCD measurements, the magnitude of the magnetization can

also be quantitatively determined.

For domain imaging, the magnetic x-ray dichroism is monitored 1) by measuring the total

electron yield (Stöhr et al, 1993; Tonner et al, 1994; Schneider, 1996) or 2) in the case of thin

samples, by directly measuring the transmitted x-ray flux (Fischer et al, 1996). In the first

method, the secondary electrons emitted from the magnetic material are electron-optically

imaged onto a channel plate. The intensity in this magnified image is proportional to the x-rays

absorbed at the point where the electrons originate and therefore on the relative orientation of the

magnetization and the photon helicity at that point. Thus, XMCD gives a spatially resolved

image of the magnetization direction. In the second method, the differential x-ray absorption is

imaged in a transmission x-ray microscope to give the magnetization image. In either imaging

mode, the image shows the projection of the magnetization along the photon propagation

direction. In the electron imaging mode the surface is illuminated at oblique incidence so the in-

plane magnetization is predominantly imaged. In the transmission mode, the magnetization

perpendicular to the sample surface is measured.

Recently, x-ray magnetic linear dichroism (XMLD) has also been observed (Hillebrecht et al,

1995). The difference in the absorption of linearly polarized x-rays is the x-ray analog of the

transverse (magnetization perpendicular to the plane of incidence) magneto-optic Kerr effect.

Although the image contrast obtained with linearly polarized light is about ten times less than

with circularly polarized light, an image of the magnetization orthogonal to the light direction

can be measured.

Practical Aspects of the Method

The lateral best spatial resolution achieved to date in the electron imaging mode is 200 nm.

Typical resolution is approximately 500 nm. Magnetization images of a monolayer thick

magnetic film can be obtained. Changes in images can be observed in real time on a video

monitor; acquisition time for a high quality image is a few minutes. An image of recorded bits

on a Co-Pt magnetic hard disk derived from the magnetic dichroism at the Co L-edge is shown in

Fig 1. If the incident x-ray energy is tuned away from the absorption edges, the dichroism is

absent and a secondary electron image of the topography is obtained. The non-uniform response

of the optical system can be removed by normalizing to this topography image. The acquisition

time and lateral resolution can be improved with increased synchrotron radiation flux which is

becoming available from insertion devices on new higher power storage rings. The ultimate

resolution would then be limited by the resolution of the imaging electron optics which has been

demonstrated at 10 nm in low energy electron microscopy (LEEM) as discussed in the next

section.

Transmission XMCD (TXMCD) is an even more recent development. The lateral spatial

resolution achieved in the first magnetic imaging experiments was 60 nm. Spatial resolution of

20 nm can be achieved in a transmission x-ray microscope. Information is provided about the

bulk properties integrated over the path of the transmitted x-rays through the sample. In contrast

to the electron imaging mode, there are no constraints on the application of magnetic fields. A

1024 x 1024 pixel image can be acquired in 3 sec.

The equipment for magnetic imaging in either mode involves sophisticated electron or x-ray

optics and would be considered complex. The cost is approximately $300K not including the

required synchrotron radiation beam line.

Method Automation

Magnetic domain imaging using XMCD in either the electron imaging or transmission mode can

be automated in the sense that the incident wavelength variation and image acquisition are under

computer control; in principle both methods could be set up for automatic data acquisition over

several hours. In reality, however, both methods are sufficiently new that their application

should not be considered routine or automatic.

Data Analysis and Initial Interpretation

There is sufficient contrast in XMCD that domains can be seen in the raw images as they are

acquired. The contrast can be improved by subtracting properly scaled images taken at the L_2

and L_3 edges. This also removes possible artifacts due to topography which can be present in the electron images. Using the elemental specificity of XMCD it is possible to measure separately the contributions of different elements in a complicated system to the magnetization image.

Sample Preparation

The sample preparation requirements are somewhat different in the two imaging modes. For electron imaging, the sample should be conductive; for an insulator, it should be not more than approximately 100 nm thick. The information sampling depth is material dependent; it is about 2 nm for transition metals and on the order of 10 nm in insulators. Even though the sampling depth for a transition metal ferromagnet is fairly short, there are no strict requirements on sample cleanliness, because the relative intensity of the secondary electrons is unchanged as they exit through a surface contamination layer such as carbon. Magnetic images can be obtained from surfaces with an rms roughness on the order of 100 nm.

A major consideration in the transmission imaging mode is the sample thickness which should be selected for 30-40% x-ray transmission which implies thicknesses on the order of 100 nm for transition metals. Because magnetic microstructure is thickness dependent, this imaging technique is particularly well suited when the sample to be measured is of the appropriate thickness. On the positive side, the sample need not be conducting, and the measurement is insensitive to surface contamination or moderate roughness.

Spin Polarized Low Energy Electron Microscopy (SPLEEM)

Principles of the Method

Low energy electron microscopy (LEEM) is a relatively new technique for surface imaging that

uses electron lenses as in conventional electron microscopes to image elastically backscattered

low energy (1-100 eV) electrons (Bauer, 1994, 1996). In the case of crystalline samples, contrast

is most often produced by diffraction . Other contrast mechanisms include interference in

overlayers or between terraces of different height on the surface. Topographic features can be

resolved with submonolayer vertical resolution and lateral resolution of 5-10 nm. In addition to

measurements of surface topography, LEEM has been used to study phase transitions,

sublimation and growth, and the interaction of the surface with foreign atoms such as adsorbates

or segregated species. A particular strength of LEEM is its rapid image acquisition over a large

field of view (5-10 micrometers diameter), which allows surface processes to be observed in real

time.

Magnetic contrast can be obtained by replacing the conventional electron gun with a spin

polarized electron gun that produces a beam of electrons with a preferential orientation of the

electron spins. In such a spin polarized low energy electron microscopy (SPLEEM)

measurement, there is an additional interaction, the exchange interaction, between the incident

electron spin $\mathbf{s}$ and the net spin density of a ferromagnetic or ferrimagnetic material. The

contribution to the scattering resulting from the exchange interaction is proportional to $\mathbf{s} \cdot \mathbf{M}$,

where $\mathbf{M}$ is the sample magnetization. The spin dependent scattering is largest at an energy near

a band gap in the spin-split band structure such that electrons of one spin but not the other are

reflected. The greatest magnetic sensitivity is achieved by reversing the electron spin

polarization direction in order to measure the normalized difference between the intensity $I^{\uparrow\uparrow}$

with $\mathbf{s}$ and $\mathbf{M}$ parallel and $I^{\uparrow\downarrow}$ with $\mathbf{s}$ and $\mathbf{M}$ antiparallel. This normalized spin dependent

asymmetry $A = (I^{\uparrow\uparrow} - I^{\uparrow\downarrow})/(I^{\uparrow\uparrow} + I^{\uparrow\downarrow})$ has the advantage that it is independent of, but correlated

with, the topographic contrast, $I^{\uparrow\uparrow} + I^{\uparrow\downarrow}$, that is measured independently at the same time.

Examples of a magnetic and topographic image are shown in Fig. 5. In a typical magnetic

material, the magnitude of the magnetization is constant, but the direction varies from one

domain to another or within a domain wall. Using a spin rotation device in the incident beam, it

is possible to get a quantitative measurement of the direction of the magnetization in a SPLEEM

image.

Practical Aspects of the Method

SPLEEM is applicable to ferromagnetic or ferrimagnetic materials, that is, materials with a net

spin density. With electrons as the probe, samples should have sufficient conductivity to avoid

charging. The sensitivity is such that domains in as little as two monolayers (ML) of Co can be

imaged at a lateral resolution of 40 nm. The best spatial resolution demonstrated for SPLEEM at

the present time is about 20 nm. Changes in the magnetization can be observed in real time as

other parameters such as temperature or film thickness are changed. Application of a magnetic

field is usually not practical because a stray field would disturb the low energy electrons

involved in the imaging. The dynamical imaging frequency is approximately 1 Hz. The

acquisition time for an 8 bit 512 x 512 pixel image of, for example 5 ML Co, is 1-3 s. The

technique is developing and the resolution improving with the further development of a rather

special objective lens, a cathode lens in which the specimen is one of the electrodes.

Method Automation

Data is usually acquired by measuring the difference between the images taken for opposite directions of the incident electron beam polarization. Imaging can be automated in the sense that the digital image can be obtained as conditions, e.g., temperature or spin polarization direction of the incident beam, are varied under computer control.

Data Analysis and Initial Interpretation

From any particular SPLEEM image, one gets a picture of the magnetization along the chosen direction of spin polarization. By rotating the incident polarization, one can obtain a measure of the three components of the magnetization, M_x, M_y, and M_z, which are proportional to the asymmetries A_x, A_y, and A_z measured along each spin polarization direction. The distribution of magnetization directions can be plotted and analyzed in light of, for example, anisotropies expected to determine the magnetization direction. A consistency check on the data is obtained by computing the relative magnitude of the magnetization, $M=(M_x^{\,2}+M_y^{\,2}+M_z^{\,2})^{1/2}$, which is expected to be constant over the image.

Sample Preparation

Because low energy electrons are central to this measurement, it is surface sensitive with an energy and material dependent probing depth that ranges from a few monolayers to approximately 10 monolayers. The experiment therefore takes place in ultrahigh vacuum and the usual surface science techniques are used to prepare a clean surface. Because of the longer probing depths at very low energies, it may be possible to obtain an image from a surface covered by an adsorbate monolayer if the adsorbate does not affect the magnetization. Most

magnetic materials are not adversely affected by low energy electron beams. This technique is well suited for *in situ* ultra high vacuum measurements such as the observation of the development of magnetic domains as a function of film thickness.

Scanning Hall Probe and Scanning SQUID Microscopes

Principles of the Method

Scanning Hall (Chang et al, 1992; Oral et al, 1996) and scanning Superconducting Quantum Interference Device (SQUID) techniques (Kirtley et al, 1995) give quantitative measurements of the stray magnetic field perpendicular to and just outside a surface. Each has been demonstrated for domain imaging although originally designed for measurement of magnetic flux in superconductors. Neither is commercially available and with the limited spatial resolution demonstrated to date, the choice of either of these techniques would likely be driven by the need for non-invasive quantitative measurements with high sensitivity. Both the Hall and SQUID probes use scanning tunneling microscopy positioning techniques to achieve close proximity to the surface and for scanning.

Practical Aspects of the Method

The scanning Hall probe is more versatile than the SQUID. It consists of a submicron Hall sensor, manufactured in a two-dimensional electron gas, and gives a voltage output proportional to the magnetic field perpendicular to the sensor. It has been operated from liquid He temperature to room temperature (with a reduction in sensitivity) and does not have a limitation on the ambient magnetic field. Typical spatial resolution is 1000 nm and the best resolution achieved is 350 nm. The magnetic field sensitivity depends on the speed or bandwidth of the

measurement. At a temperature of 77 K, the sensitivity is 3×10^{-8} T/(Hz)$^{1/2}$ times the square root of the bandwidth given in Hz. Hence, a measurement with a sensitivity of 3×10^{-6} T is possible with a 10 kHz bandwidth. High spatial and magnetic field resolution images require a few minutes. Lower resolution images can be acquired in a few seconds. The scanning SQUID is typically operated at liquid He temperature in low (less than 8 kA/m) ambient magnetic fields. A spatial resolution of 10 micrometers has been demonstrated with a magnetic field sensitivity of 10^{-10} T/Hz$^{1/2}$.

Literature Cited

Argyle, B. E., 1990, A magneto-optic microscope system for magnetic domain studies, in *Proc. Electr. Chem. Soc. Symposium on Magnetic Materials and Devices*, Vol 90-8 (L.T. Romankiw and D. A. Herman Eds.), pp 85-95

Bauer, E. 1994. Low energy electron microscopy, *Rep. Prog. Phys.* 57: 895-938.

Bauer, E. 1996. Low energy electron microscopy. *In* Handbook of Microscopy, (S. Amelinckx, D. van Dyck, J. F. van Landuyt, and G. van Tendeloo, eds.) VCH Verlagsges., Weinheim.

Betzig, E., Trautman, J. K., Wolfe, R., Gyorgy, E. M., Finn, P. L., Kryder, M. H., and Chang, C. H., 1992, Near-field magneto-optics and high density data storage, *Appl. Phys. Lett.* **61(2)**, 142-144

Chang, A. M., Hallen, H. D., Harriott, L., Hess, H. F., Kao, H. L., Kwo, J., Miller, R. E., Wolfe, R., van der Ziel, J., and Chang, T. Y. 1992. Scanning Hall probe microscopy, *Appl. Phys. Lett.* 61: 1974-1976.

Chapman, J. N. 1984, The investigation of magnetic domain structures in thin film foils by electron microscopy, *J. Phys. D: Appl. Phys.*, 17:623-47.

Craik, D. J., 1974, The Observation of Magnetic Domains, in Methods of Experimental Physics

Vol. 11, (R. V. Coleman ed.), pp. 675-743, Academic Press, New York

Du, M., Xue, S. S., Epler, W., and Kryder, M. H., 1995, Dynamics of the domain collapse in the true direct overwrite magneto-optic disk, *IEEE Trans. Magn.* **31**, (1995) 3250-3252

Fischer, P., Schütz, G., Schmahl, G., Guttmann, P., and Raasch, D. 1996. Imaging of magnetic domains with the X-ray microscope at BESSY using X-ray magnetic circular dichroism, *Z. Phys. B* 101: 313-316.

Goto, K. and Sakurai, T., 1977, A colloid-SEM method for the study of fine magnetic domain structures, *Appl. Phys. Lett.* **30 (7)**, 355-356

Heyderman, L. J., Chapman, J. N., Gibbs, M. R. J. and Shearwood, C. 1995, Amorphous melt spun ribbons and sputtered thin films - investigation of the magnetic domain structures by TEM, *J. Mag. Mag. Matrls.* 148:433-445.

Hillebrecht, F. U., Kinoshita, T., Spanke, D., Dresselhaus, J., Roth, Ch., Rose, H. B., and Kisker, E. 1995. New magnetic linear dichroism in total photoelectron yield for magnetic domain imaging, *Phys. Rev. Lett.* 75: 2224-2227.

Hubert, A. and Schäfer, R., 1998, Magnetic Domains: the Analysis of Magnetic Microstructures, Springer, Berlin

Hug, H. J., Stiefel, B. van Schendel, P. J. A., Moser, A., Hofer, R., Güntherodt, H.-J., Porthun, S. Abelmann, L., Lodder, J. C., Bochi, G. and O'Handley, R. C. 1998. Quantitative Magnetic Force Microscopy on Perpendicularly Magnetized Samples", *J. Appl. Phys.* 83:5609-5620

Kelley, M.H., Unguris, J., Scheinfein, M.R., Pierce,, D. T., and Celotta, R. J. 1989. Vector Imaging of Magnetic Microstructure. *In* Proceedings of the Microbeam Analysis Society Meeting (P. E. Russell, ed.) pp. 391-395. San Francisco Press, San Francisco, Calif.

Kirilyuk, V., Kirilyuk, A., and Rasing, Th., 1997, New mode of domain imaging: Second harmonic generation microscopy, *J. Appl. Phys.* **81**(8) 5014-5015.

Kirtley, J. R., Ketchen, M. B., Tsuei, C. C., Sun, J. Z., Gallagher, W. J., Yu-Jahnes, L. S., Gupta, A., Stawiasz, K. G., and Wind, S. J. 1995. Design and applications of a scanning SQUID microscope, *IBM J. Res. Develop.* 39: 655-668.

Kitakami, O., Sakurai T., and Shimada, Y., 1996, High density recorded patterns observed by high-resolution Bitter scanning electron microscope method, *J. Appl. Phys.* **79** (8), 6074-6076

Kittel, C. and Galt, J. K., 1956, Ferromagnetic Domain Theory, in Solid State Physics Vol. 3, (F. Seitz and D. Turnbull Eds.), pp. 437-564, Academic Press, New York

Mankos, M., Cowley, J. M., and Scheinfein, M. 1996, Quantitative micromagnetics at high spatial resolution using far-out-of-focus STEM electron holography, *Phys. Stat. Sol. (a)* 154:469-504.

Mankos, M., Scheinfein, M. R., and Cowley, J. M. 1996, Electron Holography and Lorentz Microscopy of magnetic materials, *Advances in Imaging and Electron Physics* 98:323-426.

McFadyen, I. R. and Chapman, J. N. 1992, Electron microscopy of magnetic materials, *Electron Microscopy Society of America Bulletin* 22:64-75.

McVitie, S. and Chapman, J. N. 1997, Reversal mechanisms in lithographically defined magnetic thin film elements imaged by scanning transmission electron, *Microsc. Microanal.* 3:146-153.

Newbury, D. E., Joy, D. C., Echlin, P., Fiori, C. E., Goldstein, J. I. 1986. Advanced Scanning Electron Microscopy and X-Ray Microanalysis. Plenum Press, New York, NY.

Nikitenko, V. I., Gornakov, V. S., Dedukh, L.M., Kabanov, Yu. P., Khapikov, A. F., Bennett, L. H., Chen, P. J., McMichael, R. D., Donahue, M. J., Swartzendruber, L. J., Shapiro, A. J. , Brown, H. J., and Egelhoff, W. F., 1996, Magneto-optical indicator film study of the magnetization of a symmetric spin valve, *IEEE Trans. Magn.* **32**(5) 4639-4641

Oral, A., Bending, S. J., and Henini, M. 1996. Real-time scanning Hall probe microscopy, *Appl. Phys. Lett.* 69: 1324-1327.

Osakabe, N., Yoshida, K., Horiuchi, Y., Matsuda, T., Tanabe, H., Okuwaki, T., Endo, J., Fujiwara, H., and Tonomura, A. 1983, Observation of recorded magnetization pattern by electron holography, *Appl. Phys. Lettr.* 42:746-748.

Petek, B., Trouilloud, P. L., and Argyle, B., 1990, Time-resolved domain dynamics in thin-film heads, *IEEE Trans. Magn.* **26**(5) 1328-1330

Reimer, L. 1985. Scanning Electron Microscopy. Springer-Verlag, Berlin.

Rugar, D. and Hansma, P. 1990. Atomic Force Microscopy. *Physics Today*, 43(10):23-30.

Sarid, D. 1991. Scanning Force Microscopy. Oxford University Press, New York, NY.

Scheinfein, M.R. , Unguris, J., Kelley, M.H., Pierce, D. T., and Celotta, R. J. 1990. Scanning Electron Microscopy With Polarization Analysis (SEMPA). *Rev. Sci. Instrum.* **61:**2501-2506.

Schmidt, F., Rave, W., and Hubert, A., 1985, Enhancement of magneto-optical domain observation by digital image processing, *IEEE Trans. Magn.* **21**(5), 1596-1598

Schneider, C. M. 1996. Imaging magnetic microstructures with elemental selectivity: application of magnetic dichroisms. In Spin-Orbit Influenced Spectroscopies of Magnetic Solids, (H. Ebert and G. Schütz, eds.) pp. 179-196, Springer-Verlag, Berlin.

Schoenenberger, C., Alvarado, S. F., Lambert, S. E., and Sanders, I. L. 1990. Separation of Magnetic and Topographic effects in Force Microscopy. *J. Appl. Phys.*, 67:7278-7280.

Silva, T.J. and Kos, A. B., 1997, Nonreciprocal differential detection method for scanning Kerr-effect microscopy, *J. Appl. Phys.* **81** (8), 5015-5017

Silva, T.J. and Schultz, S., 1996, A scanning near-field optical microscope for the imaging of magnetic domains in reflection, *Rev. Sci. Instrum.* **67**(3), 715-725

Stöhr, J., Wu, Y., B. Hermsmeier, D., Samant, M. G., Harp, G. R., Koranda, S., Dunham, D., and Tonner, B. P. 1993. Element-specific magnetic microscopy with circularly polarized X-rays, *Science* 259: 658-661.

Tonner, B. P., Dunham, D., Zhang, J., O'Brien, W. L., Samant, M., Weller, D., Hermsmeier, B. D., and Stöhr, J. 1994. Imaging magnetic domains with the X-ray dichroism photoemission microscope, *Nucl. Instrum. Meth. A* 347: 142-147.

Tonomura, A. 1994, Electron Holography, Springer-Verlag, Berlin.

Trouilloud, P. L., Petek, B. Argyle, B. E., 1994, Methods for wide-field Kerr imaging of small magnetic devices, *IEEE Trans. Magn.* **30**(6), 4494-4496

Wells, O. C., 1983, Fundamental theorem for type-1 magnetic contrast in the scanning electron-microscope (SEM), *J. Microscopy-Oxford* 131, RP5-RP6

Figure Captions

Figure 1. An illustration of several magnetic imaging techniques using a pattern written on magnetic storage media. The test pattern is composed of horizontal tracks, each about 10 μm wide and containing a series of magnetization reversals, or "bits". The bit length ranges from 10.0 to 0.2 μm. The bit length and spacing of the large bits in the XMCD electron yield image is 10 μm (Tonner et al, 1994). Note: the Bitter and XMCD images are from a different, but similar, test sample.

Figure 2. Magneto-optic image of a thin film recording head. The lower panel shows the raw optical image showing the sample topography. The top panel shows the difference between two magneto-optical images taken with opposite currents driving the head magnetization. The white and black regions reveal how the domain walls have moved. The head is about 100 μm across. (Photo courtesy of B. Argyle)

Figure 3. Top: A Fresnel image of a metallic glass magnetic material showing a bright and a dark domain wall. Bottom: A Foucault image of the same area where the contrast depends on the magnetization parallel to the domain walls, as indicated by the arrows. In addition to the main 180° domains, these techniques clearly reveal small variations in the magnetization, i.e., magnetization ripple. (Heyderman et al, 1995)

Figure 4. Top: A schematic diagram showing an inductive recording head writing domains of in-plane magnetization on a magnetic recording tape. Bottom: An interference micrograph, obtained using
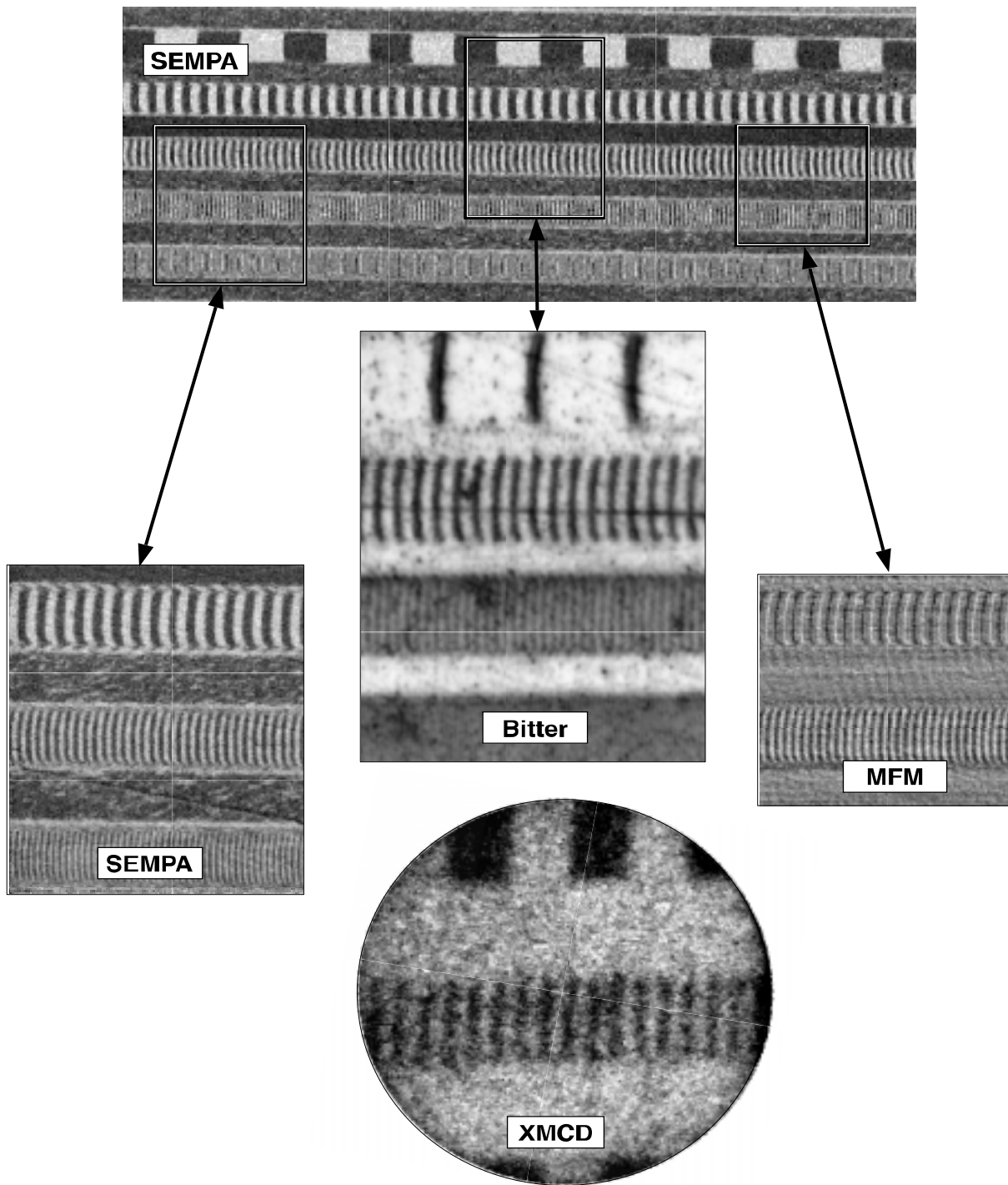
electron holography, illustrating the flux distribution both outside (top 25% of image) and inside

(bottom 75%) this image of a 45 nm thick Co film. (Osakabe, 1983)

Figure 5. a) SPLEEM image of 5 monolayer thick Co film on a W(110) single crystal surface. The

polarization is in plane and collinear with the uniaxial magnetization. Taken at an energy of 1.5 eV, to

optimize the magnetic contrast, with a field of view of 8 μm. b) LEEM image of the same region at an

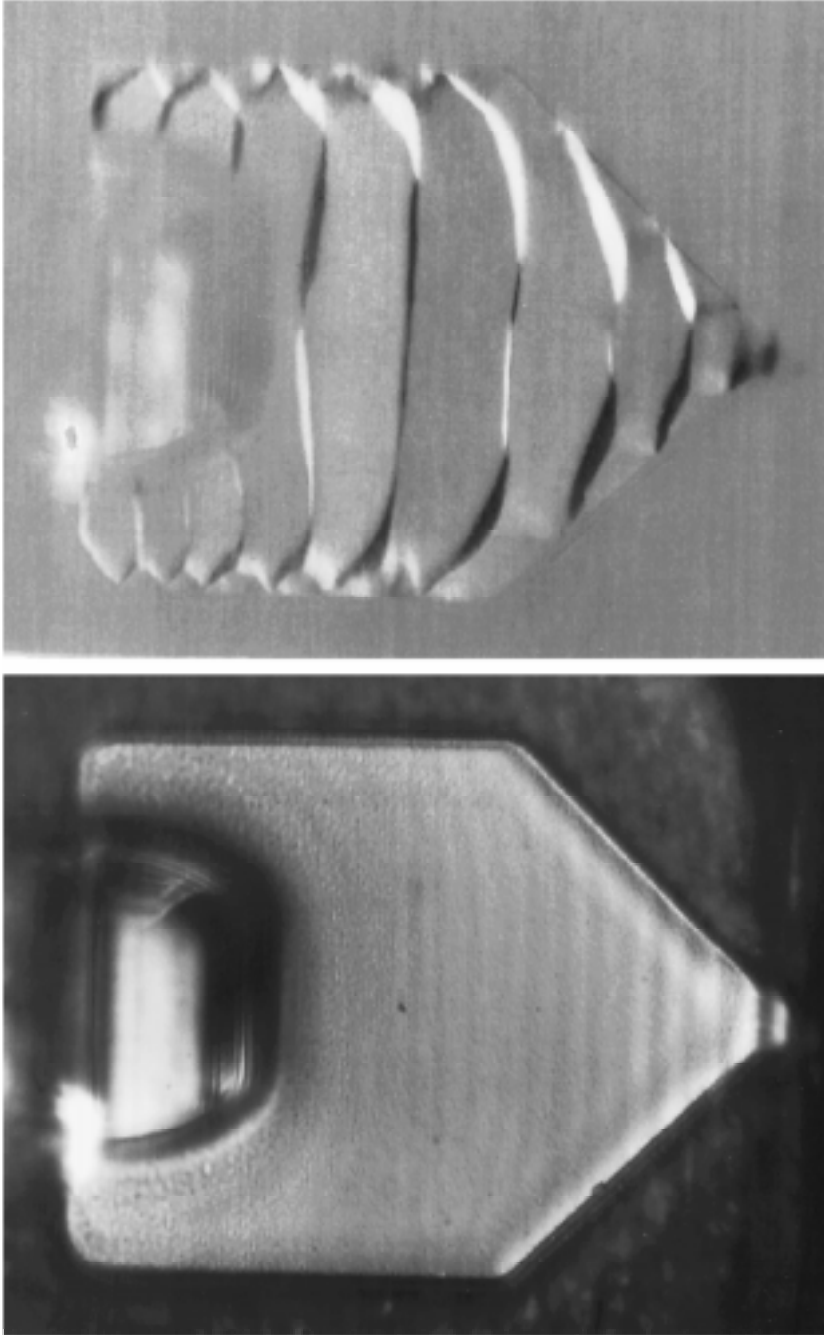energy of 3.6 eV showing the atomic scale roughness of the Co film. (Courtesy of E. Bauer)

Table 1	Bitter	Magneto-optic	MFM	Lorentz	DPC	SEMPA	Holography	XMCD	TXMCD	SPLEEM
Principles of method										
Contrast Origin	grad $B_{ext.}$	**M**	grad $B_{ext.}$	**B**	**B**	**M**	**B, Φ_B**	**M**	**M**	**M**
Quantitative	No	Yes	No	Yes	Yes	Yes	Yes	Yes	Yes	Yes
Practical Aspects										
Best Resolution (nm)	100	300	40	~10	~2	20	~5	300	30	20
Typical Resolution (nm)	500	1000	100	50	20	200	20	500	60	40
Information Depth (nm)	500	20	20 - 500	Sample Thickness	Sample Thickness	2	Sample Thickness	2 - 20	Sample Thickness	1
Acquisition Time	.03 sec.	10^{-8} - 1 sec.	5 - 30 minutes	0.04-30 sec.	5-50 sec.	1 - 100 minutes	.03-10 sec.	.03 sec. to 10 minutes	3 sec	1 sec
Insulators	Yes	Yes	Yes	No	No	No	No	Yes	Yes	No
Vacuum Requirement	None	None	None	HV	HV	UHV	HV	UHV	None	UHV

Complexity	Low	Moderate	Moderate	Moderate	Mod./High	High	High	High	High	High
Commercially Available	Yes	Yes	Yes	Yes	No	No	Yes	No	No	No
Cost	1 K$	50-500 K$	150 K$	0.2-1 M$	1 M$	800 K$	1.3 M$	300+ K$	300+ K$	1 M$
Sample Prep										
Sample thickness (nm)	No Limit	No Limit	No Limit	<150	<150	No Limit	<150	No Limit	< 100	No Limit
Special Smoothness	Yes	Yes	Yes	Yes	Yes	No	Yes	No	Yes	Yes
Clean Surface Required	No	No	No	No	No	Yes	No	No	No	Yes
Specimen Modification										
Maximum Applied External Field (kA/m)	No Limit	No Limit	800	500 (vert.) 100 (horiz.)	500 (vert.) 100 (horiz.)	None	100	None	No Limit	None
Problems										
Topographic Feedthrough	Yes	Yes	Yes	Some	Some	No	Some	No	No	No
Crystallographic	No	No	No	Yes	Yes	No	Yes	No	Not	Yes

|									
Feedthrough								Tested	

Figure 1: An illustration of several magnetic imaging techniques using a pattern written on magnetic storage media. The test pattern is composed of horizontal tracks, each about 10 μm wide and containing a series of magnetization reversals, or "bits". The bit length ranges from 10.0 to 0.2 10 μm. The bit length and spacing of the large bits in the XMCD electron yield image is 10 μm (Tonner et al, 1994). Note: The Bitter and XMCD images are from a different, but similar, test sample.
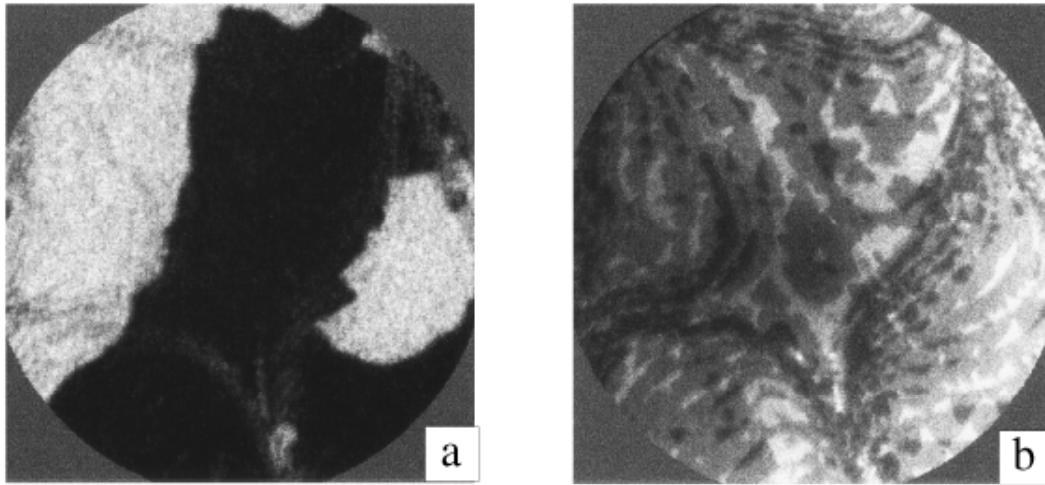
Figure 2 Magneto-optic image of a thin film recording head. The lower panel shows the raw optical image showing the sample topography. The top panel shows the difference between two magneto-optical images taken with opposite currents driving the head magnetization. The white and black regions reveal how the domain walls have moved. The head is about 100 μm across. (Photo courtesy of B. Argyle)

Figure 3 Top: A Fresnel image of a metallic glass magnetic material showing a bright and a dark domain wall. Bottom: A Foucault image of the same area where the contrast depends on the magnetization parallel to the domain walls, as indicated by the arrows. In addition to the main 180° domains, these techniques clearly reveal small variations in the magnetization, i.e., magnetization ripple. (Hyderman et al, 1995)
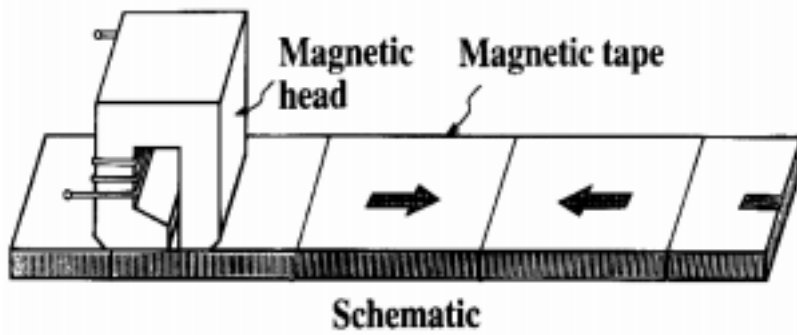
Figure 4 Top: A schematic diagram showing an inductive recording head writing domains of in-plane magnetization on a magnetic recording tape. Bottom: An interference micrograph, obtained using electron holography, illustrating the flux distribution both outside (top 25% of image) and inside (bottom

Figure 5 a) SPLEEM image of 5 monolayer thick Co film on a W(110) single crystal surface. The polarization is in plane and collinear with the uniaxial magnetization. Taken at an energy of 1.5 eV, to optimize the magnetic contrast, with a field of view of 8 μm. b) LEEM image of the same region at an energy of 3.6 eV showing the atomic scale roughness of the Co film. (Courtesy of E. Bauer)